IFT-P.023-93
Fermilab Library
0 1160 0029766 7

IFT

Instituto de Física Teórica
Universidade Estadual Paulista

April/93

IFT-P.023/93
CU-TH-593

2D χ^2 Analysis of Pion Interferometry Data from the AGS *

Miklos Gyulassy[1]

Physics Department
Columbia University
New York, N.Y. 10027

and

Sandra S. Padula[2]

Instituto de Física Teórica
Universidade Estadual Paulista
Rua Pamplona, 145
01405-900 - São Paulo, S.P.
Brazil

*This work was supported by the Director, Office of Energy Research, Division of Nuclear Physics of the Office of High Energy and Nuclear Physics of the U.S. Department of Energy under Contract No. De-FG02-93ER40764.

1. Presented at the HIPAGS'93 Workshop, MIT, Jan.13-15,1993.

2. Partially supported by Conselho Nacional de Desenvolvimento Científico e Tecnológico (CNPq), Brazil.

Instituto de Física Teórica
Universidade Estadual Paulista
Rua Pamplona, 145
01405-900 – São Paulo, S.P.
Brazil

Telephone: 55 (11) 251-5155
Telefax: 55 (11) 288-8224
Telex: 55 (11) 31870 UJMFBR
Electronic Address: LIBRARY@IFT.UESP.ANSP.BR
47553::LIBRARY

CU-TH-593
IFT-P.023/93

2D χ^2 Analysis of Pion Interferometry Data from the AGS*

Miklos Gyulassy[1] and Sandra S. Padula[2,3]

Physics Department
Columbia University
New York, N.Y. 10027

Abstract:
Recent E802 pion correlation data on central Si+Au reactions at 14.6 AGeV/c are analyzed. We show that the projected one dimensional pion correlation functions are consistent with widely different decoupling space-time geometries due to uncertainties in the long lived resonance production. In particular $R_\perp = \tau = 4.6$ fm without resonances and $R_\perp = 3.5\ \tau = 2$ fm with Lund resonance abundance provide equally good descriptions of the $C(q_\perp)$ data. To test the enhanced sensitivity of two dimensional correlation functions to the underlying dynamics, we perform a 2D χ^2 analysis of $C(q_\perp, q_L)$. We find an unexpected ridge of high χ^2 along $q_\perp = q_L$ due to systematic tilting of the experimental correlation function upward in the $(q_\perp, q_L)$ plane. Even after including that extra degree of freedom, however, the minimum χ^2 geometries are found to provide only a poor fit. We discuss future work required to improve this situation. Finally, we review the advantages of kaon interferometry and discuss novel aspects of $K_s K_s$ interferometry as a probe of strangeness distillation.

1 Introduction

Pion and kaon interferometry aims to exploit interference effects caused by Bose symmetrization to probe the space-time geometry of high energy hadronic and nuclear reactions. In this work, we report recent results of a continuing study [1]-[5] of like-pion or like-kaon correlation functions,

$$C_n(\mathbf{k}_1, \cdots, \mathbf{k}_n) = \mathcal{N}_n P_n(\mathbf{k}_1, \cdots, \mathbf{k}_n) / \prod_{i=1}^{n} P_1(\mathbf{k}_i) \ , \tag{1}$$

*This work was supported by the Director, Office of Energy Research, Division of Nuclear Physics of the Office of High Energy and Nuclear Physics of the U.S. Department of Energy under Contract No. DE-FG02-93ER40764.

1. Presented at the HIPAGS '93 Workshop, MIT, Jan.13-15,1993.
2. Permanent address: IFT/UNESP, Rua Pamplona 145, 01405-900 Sao Paulo, SP, Brazil
3. Partially supported by Conselho Nacional de Desenvolvimento Científico e Tecnológico (CNPq), Brazil

where P_n denotes the n (identical) boson inclusive distributions, and $\mathcal{N}_n$ is the inverse of the normalized n^{th} factorial moment of the multiplicity distribution. We have emphasized in [2] that a direct geometrical interpretation of the interference pattern is only possible in the semi-classical limit and in the absence of correlations between the spatial and momentum coordinates. Only in such idealized cases is $C_2(\mathbf{k}_1, \mathbf{k}_2)$ directly related to the space-time density, $\rho(x)$, of pion emission points through

$$C_2(\mathbf{k}_1, \mathbf{k}_2) = 1 + \lambda |\rho(k_1 - k_2)|^2 \ , \tag{2}$$

where $\rho(q) = \int d^4x e^{iqx} \rho(x)$, and where the incoherence or chaoticity parameter $\lambda = 1$. However, in all actual cases involving high energy reactions, strong correlations between $\mathbf{x}$ and $\mathbf{k}$ exist which distort the interference pattern. The analysis of correlation functions can therefore only be performed in the context of specific dynamical models. Even though model independent analysis is not possible, the analysis of small relative momentum pion and kaon correlations is important because those correlations are sensitive to the ***phase space correlations*** predicted by transport models[7, 8], which are otherwise not tested in other inclusive measurements.

In Ref.[2] we derived via the Wigner density formalism, the interference pattern induced by Bose symmetrization for an arbitrary decoupling phase-space distribution, as predicted by Monte Carlo event generators:

$$D(x, p) = \langle \delta^4(x - x_f) \delta^4(p - p_f) \rangle \ , \tag{3}$$

where (x_f, p_f) are the phase space coordinates of the pions (or kaons) at their decoupling times x_f^0. Note that D is normalized as $\int d^4x d^4p D(x, p) = 1$. We emphasize that D does NOT correspond to the one body phase space density, $f(\mathbf{x}, \mathbf{p}, t)$, at any one time, t, because the production and final interaction times of the pions fluctuates over a wide range. Neglecting dynamical two particle correlations but allowing arbitrary correlations among the eight phase space coordinates, the n-pion inclusive distribution function can be expressed as[2, 3]

$$P_n(k_1, ..., k_n) = \sum_\sigma \prod_{i=1}^{n} G(k_i, k_{\sigma_i}) \ , \tag{4}$$

where $\sigma = (\sigma_1, ..., \sigma_n)$ runs over the $n!$ permutations of indices. Including Coulomb distortions, the two-particle correlation function reduces to

$$C(k_1, k_2) = \chi(q) \left(1 + \frac{|G(k_1, k_2)|^2}{G(k_1, k_1) G(k_2, k_2)} \right) \ . \tag{5}$$

where $\chi(q) = (q_c/q)/(e^{q_c/q} - 1)$ is the Gamow factor with $q_c = 2\pi\alpha m$ and $q = (-(k_1 - k_2)^2)^{1/2}$.

The complex amplitude $G(k_1, k_2)$ is a wavepacket smoothed Fourier transform of D given by

$$G(k_1, k_2) = \int d^4x d^4p D(x, p) e^{iqx} e^{q^2 \Delta x^2/2} e^{(p-K)^2/2\Delta p^2} \propto \langle e^{iqx_f} e^{-Kp_f/\Delta p^2} \rangle \ , \tag{6}$$

where Δp is the rms uncertainty in the final momentum of the particle at decoupling for a minimal Gaussian wavepacket with $\Delta x \Delta p = 1/2$ and $q = k_1 - k_2$ and $K = \frac{1}{2}(k_1 + k_2)$. The last form above is particularly well suited to Monte Carlo calculations which produce

a sequence of discrete points (x_f, p_f) corresponding to the last interaction point and final momentum of each particle, event by event. The interference pattern obviously depends not only on the break-up phase-space distribution, $D(x,p)$, but in general also on the quantal production dynamics characterized by Δp. In the true semi-classical limit the inclusive distributions become independent of Δp. However, this must be tested in every case by varying that parameter.

The effects of long lived resonances can also be included in the semi-classical approximation[1, 2]. Note that the pion freeze-out coordinates, x_f^μ, is related to its parent resonance freeze-out coordinates, x_r^μ, through $x_f = x_r + u_r\tau$, where u_r^μ is the resonance four velocity at break-up and τ is the proper time of its decay. Summing over resonances r of widths Γ_r, and averaging over their decay proper times, we obtain finally

$$G(k_1,k_2) \approx \langle \sum_r f_{\pi^-/r}\,(1 - iqu_r/\Gamma_r)^{-1} \exp(iqx_r - Kp_r/\Delta p^2)\rangle \ , \tag{7}$$

where $f_{\pi^-/r}$ is the fraction of the observed π^-'s arising from the decay of a resonance of type r.

In terms of G, the single inclusive distribution is $P_1(\mathbf{k}) \propto G(k,k)$. Therefore, the width Δp of the wavepackets is constrained by the measured width of the single inclusive distributions. The longitudinal momentum width grows as $\sqrt{s}$ at high energies and thus all dependence on Δp_z drops out in that limit. However, the limited transverse momentum leading to $\langle p_\perp\rangle \sim 0.3$ GeV/c provides a severe constraint on $\Delta p_\perp \ll \langle p_\perp\rangle$. Of course we cannot take $\Delta p_\perp = 0$ either because, in order to resolve a given $R_\perp$ we must have $\Delta x_\perp \sim 1/\Delta p_\perp \ll R_\perp$. Thus, the dependence of the quantal dynamics only drops out if $1/R_\perp \ll \Delta p_\perp \ll \langle p_\perp\rangle$. In practice this requires $R \gg 1$ fm. In the true semiclassical limit, $R_\perp\langle p_\perp\rangle \gg 1$ and we do not have to consider such quantal details. Unfortunately in high energy reactions with strongly correlated spatial-momentum correlations, this dependence on quantal aspects of the production dynamics cannot be neglected.

We recall here that for a realistic inside-outside cascade distribution[3]

$$D(x,p) \propto \tau e^{-\frac{\tau_f^2}{\Delta\tau^2}}\ e^{-\frac{(y-y^*)^2}{2Y_c^2}}\ e^{-\frac{(\eta-y)^2}{2\Delta\eta^2}} e^{-x_\perp^2/R_\perp^2}\delta(E - E_{\mathbf{p}})\delta^2(\mathbf{p}_\perp) \ . \tag{8}$$

where $\tau(t,z) = (t^2 - z^2)^{\frac{1}{2}}$ is the freeze-out proper time, and

$$\eta = \tfrac{1}{2}\log((t+z)/(t-z)) \ , \ y = \tfrac{1}{2}\log((E+p_z)/(E-p_z)) \ , \tag{9}$$

are the space-time and momentum rapidity variables which are strongly correlated[1] within a range $\Delta\eta \approx 0.8$. The Gaussian rapidity distribution accounts for the non-uniform rapidity density found experimentally. The rms transverse radius, $R_\perp$, at decoupling and the rms decoupling proper time, $\Delta\tau$, are the space time geometrical parameters that we hope to extract from the interference pattern. Th transverse momentum delta function represents a specific model whereby the final observed transverse distribution is due entirely to the finite wavepackets of the produced pions!

For kinematics with $m_{\perp 1} = m_{\perp 2} = m_\perp$ and $\delta y = y_1 - y_2$ small, we showed that in this case the correlation function has the approximate analytic form

$$C(k_1,k_2) \approx 1 + \frac{1}{[1 + \frac{1}{2}m_\perp^2\Delta\tau^2\Delta y^2(\Delta\eta^2 + \frac{Y_c^2\Delta p^2}{\Delta p^2 + mm_\perp Y_c^2})]^2} \ . \tag{10}$$

It is obvious from the above that the interference pattern as a function of the rapidity difference depends then not only on the geometrical quantity, $\Delta\tau^2$, characterizing the freeze-out proper time distribution but also on the width, $\Delta\eta$ of the $\eta - y$ correlation as well on the width, Y_c of the finite rapidity distribution and the wavepacket size. The $y^*, Y_c, \Delta p$ are fortunately constrained by the measured inclusive distribution

$$P_1(k) \propto G(k,k) \propto e^{-\frac{(y-y^*)^2}{2Y_c^2}} e^{-m_\perp/T} m_\perp^{-1/2} \tag{11}$$

where $T = \Delta p^2/m$ is the effective transverse mass slope. However $\Delta\tau$ and $\Delta\eta$ are convoluted in their effect on the two particle correlations. In [3] it was shown that the correlations are rather sensitive to $\Delta\eta$ in the case that long lived resonances are ignored.

The main distortion however was shown in [1, 3] to be due to long lived resonances. The Lund model gives $f_{\pi^-/direct} \approx 0.19$, $f_{\pi^-/\rho} \approx 0.40$, $f_{\pi^-/\omega} \approx 0.16$, and $f_{\pi^-/K^*} \approx 0.09$, and $f_{\pi^-/\eta} = 0.04$, $f_{\pi^-/\eta'} = 0.046$. These ratios are relatively independent of energy in the Lund model. The data[9] on resonance production at AGS energies is unfortunately rather sparse. What exists tend to indicate much smaller resonance abundance at AGS energies.

In the present study our aim is to determine whether the two extreme dynamical models with no resonance production or full Lund resonance production can be differentiated via the two pion correlations. We try to find the optimal values of $R_\perp$ and $\tau \equiv \Delta\tau$ fixing $\Delta\eta = 0.8$ from [1, 8] and $Y_c = 0.7$, $y^*_{cm} = 0$ and $\Delta p^2/m = 0.17$ GeV from the inclusive pion distributions[10]. In both cases we insist on fixing $\lambda = 1$. As we have repeatedly emphasized in [1]-[3], any fit to data treating λ as a free parameter is to be distrusted because in any finite resolution experiment the correlation functions projected on one or two dimensional manifolds necessarily leads to $\lambda < 1$ even though $C(0,K) = 2$. By treating λ as an independent fit parameter, the fitted geometrical parameters are distorted by an amount depending on details of binning and acceptance cuts of the experiment.

The only proper way to compare a dynamical model with such projected data is to perform the projection on the theory first via

$$C_{proj}(q_T,q_L) = \frac{\int d^3k_1 d^3k_2 P_2(\mathbf{k}_1,\mathbf{k}_2)\ A_2(q_T,q_L;\mathbf{k}_1,\mathbf{k}_2)}{\int d^3k_1 d^3k_2 P_1(\mathbf{k}_1)P_1(\mathbf{k}_2)\ A_2(q_T,q_L;\mathbf{k}_1,\mathbf{k}_2)} \ , \tag{12}$$

where A_2 is the experimental binning and acceptance function. Above P_2 and P_1 are the theoretical input distributions which are filtered and distorted through the experimental cuts and acceptance. Unfortunately, the lack of knowledge of A_2 is often a source of additional error that is difficult to control. Ideally, A_2 should be a subroutine provided by the experimentalists with suitable error bars to enable an estimate of the convolution error. A limitation of the following numerical study, is that we approximate A_2 by an idealized form discussed below.

It is important to note that because of this projection, Coulomb corrections do not in general factor out of the integral. Only if the experimental resolution, A_2, as a function of $\mathbf{q}$ is much higher than the width of the Coulomb hole, $q_c = 2\pi\alpha m$, and the variation of the interference is much broader that the bin widths can such an experimental correction be done unambiguously. In general, for a particular model it is always safer to correct the theory and then integrate via (12) and compare to raw data. We will show below evidence for the non-Abelian nature of this Coulomb correction.

2 One dimensional projection $C(q_\perp)$

The new data[6] on central $Si + Au \to \pi^-\pi^- + X$ is shown in Fig. 1. The top two panels (a,b) show data corrected for acceptance but not corrected for Coulomb. The calculated curves therefore include the Gamow factor (hence labeled Gamow ON). The lower panels (c,d) show data corrected for Coulomb distortions using the mean Gamow factor for each bin in a two dimensional binning of the coincidence data followed by a projection onto the $q_\perp = |\mathbf{k}_{\perp 1} - \mathbf{k}_{\perp 2}|$ axis. The left side (a,c) shows the calculated correlation function in three different assumption about the resonance fractions assuming $R_\perp = 3.5$ fm and $\tau = 2$ fm. The three curves correspond to (1) no resonance production (direct pions only) (2) 1/10 the fraction of Lund resonances, and (3) resonance abundance as predicted via the Lund model[8]. On the right hand side (b,d) we consider another geometry with $R_T = \tau = 4.6$ fm.

All calculation were performed using the Monte Carlo importance sampling method via the CERES program developed in [1]. The acceptance function was assumed to be of idealized form

$$A_2(q_\perp; \mathbf{k}_1, \mathbf{k}_2) = A_1(\mathbf{k}_1)A_1(\mathbf{k}_2)\theta(0.005 < |k_{z1} - k_{z2}| < 0.015)\delta(q_\perp - |\mathbf{k}_{\perp 1} - \mathbf{k}_{\perp 2}|) \ , \quad (13)$$

with $\mathbf{k}_i$ in the cm frame and $A_1(\mathbf{k}) = \theta(0.35 - |y_{cm}|)\theta(0.1 < k_\perp < 0.95)$. This simplified assumption for the experimental acceptance represents a potentially major limitation of the present analysis that will have to be improved in the future.

What is most striking in Fig 1 is that by varying the resonance degree of freedom, widely different geometries seem compatible with the same data. Of course if the data is fit by a one parameter Gaussian, a unique R minimizing the χ^2 will emerge. The point of Fig. 1 is to show that if the dynamical degree of freedom involving resonance production is incorporated into the analysis, then a wide range of R and τ can be found to be compatible with the same data. This is of course the same conclusion we drew in the analysis of NA35 correlation data before in Ref.[1]. However, it bears repeating in this context especially since there is so little experimental constraint on resonance production at AGS energies.

Note also that the effective intercept in all case is less than unity. even though in all cases the theoretical $\lambda = 1$. This shows once again that λ must not be treated as an independent fit parameter. There is useful physical information in the effective intercept. It is sensitive to the variation of the correlation function in the other dimensions integrated over for this projection. In particular, we see that the full resonance fraction leads to systematically lower intercepts than no resonance dynamics in all cases. The smallest $q_\perp$ bins seem more compatible with no or 1/10 resonance cases, but the error bars on the data are too big to draw firm conclusions. With higher statistics, however, the intercept and small $q_\perp$ behavior could in principle distinguish between these extreme dynamical models.

Finally we note the effect of comparing uncorrected data to Gamow corrected theory versus comparing Coulomb corrected data with theory incorporating Coulomb distortions. Ideally, the two methods should yield similar conclusions as long as the Gamow approximation (neglecting the radial dependence of the Coulomb wavefunction on a scale R) remains valid. However, in the case of the geometry on the left side it appears that the full resonance curve fits the Coulomb corrected data on bottom significantly better than the uncorrected data on top. This is a warning signal that the operations do not commute. In this case, the only proper comparison is with respect to unmolested data on top. The Gamow distortion

is theoretically unambiguous and so should be included in the theoretical calculation. The experiment "correction" is at best approximate and should be avoided.

One may argue that the two particle acceptance correction could lead to unwanted extra distortions. This would be the case if for example $A_2(k_1, k_2) \sim 1 - \exp(-q^2/q^2_{res})$ with the two track resolution q_{res} being large. In such cases the two dimensional projected correlation function measured experimentally via (13) could not be corrected simply by dividing each $q_\perp$ and q_L bin by some averaged $A_2(k_1, k_2)$. In this worst of all worlds, it is only meaningful to compare raw data with theoretical calculation folded through the experiment acceptance function. We will not pursue the later option here due our lack of knowledge of the detailed e802 acceptance. In principle, it is trivial however to improve the calculation as information on A_2 becomes available.

3 Two Dimensional χ^2 analysis

To test whether the two dimensional $C(q_\perp, q_L)$ could be more sensitive to differences between resonance and non-resonance dynamics, we computed the standard measure of goodness of fit on a two dimensional grid in the $(q_\perp, q_L)$ plane

$$\chi^2(i,j) = \frac{(C_{exp}(i,j) - C_{th}(i,j))^2}{(\Delta C_{exp}(i,j))^2} \ . \quad (14)$$

The data $C_{exp}(i,j) \pm \Delta C_{exp}(i,j)$ are as yet unpublished and were obtained from R. Morse[13] with a clear warning of their PRELIMINARY nature. While any conclusion would be premature at this stage, we discuss here this method of analysis since it exposes a new complication that must be dealt with. In Figure 2 we show the preliminary acceptance and Coulomb corrected data in a lego plot in the kinematic region $0.005 < q_\perp < 0.125$, $0.005 < q_L < 0.105$ GeV. A clear bump at $q_\perp, q_L < 0.06$ GeV is obvious. The lower lego plot is the theoretical correlation function without Gamow corrections for the geometry $R_\perp = \tau = 4.6$ fm and no resonance production. While the bump is in the general right ballpark, the shape appears to be different, and at large $q_\perp \sim q_L \sim 0.1$ the data remain significantly above unity, where the theory is very close to unity.

Figure 3a shows the corresponding lego plot of the $\chi^2(i,j)$. The surprise is the very high ridge near $q_\perp \approx q_L$ especially in the totally uninteresting region at high $q_\perp = q_L$. On closer inspection the problem is due mainly to the small statistical errors at high $q_\perp, q_L$ that amplifies the small difference between theory and experiment in a region where $C(q_\perp, q_L) \approx 1$.

We therefore tested whether allowing for small systematic errors causing an upward tilt of $C_{exp}(q_\perp, q_L) \approx 1 + \epsilon q_\perp + \epsilon' q_L$ could be responsible for this ridge. To determine the tilt slopes ϵ, ϵ', we minimized the global error

$$\chi^2_{tilt}(\epsilon, \epsilon') \equiv \frac{1}{30} \sum_{i,j} \frac{(C_{exp}(i,j) - (1 + \epsilon q_\perp + \epsilon' q_L)C_{th}(i,j))^2}{(\Delta C_{exp}(i,j))^2} \ . \quad (15)$$

Minimization involves solving the linear system, $\partial\chi^2_{tilt}/\partial\epsilon_i = 0$.

The resulting tilted χ^2 is shown in Fig. 3b. While the tilt degree of freedom reduced considerably the height of the ridge, the residual χ^2 is still large everywhere. Averaging over

the grid, we found that for the 30 degrees of freedom

$$\langle\chi^2\rangle \approx 1.5 \times (30) \ . \tag{16}$$

The probability that this is just a statistical fluctuation is about 1/20. Therefore, we find that although in the one dimensional plot the no-resonance fit with $R_\perp = \tau = 4.6$ fm gave a very good fit to $C(q_\perp)$, it seems to be a rather poor fit in 2 dimensions.

We have varied the $R_\perp$ and τ to see if we could lower the χ^2 but failed to find a better fit. The problem is not only in the large $q_\perp, q_L$ domain where systematic experimental errors are likely the culprit, but also in the small $q_\perp, q_L < 0.04$ where all the physics is supposed to hide. Recently, R. Morse suggested that we also include an overall normalization degree of freedom in minimizing χ^2. Calculations along those lines is in progress. In addition, calculations are in progress for the tilted χ^2 for full resonance dynamics. However, it is clear that a better understanding of the systematic biases distorting the 2D correlation functions will be necessary to draw more definitive conclusions.

4 Kaon versus Pion Interferometry

In addition to ever more refined analysis of pion correlations, an independent handle on the phase-space dynamics can be obtained by studying the interference pattern of identical kaons. In Ref. [4] we showed that kaon interferometry provides a valuable complementary tool to pion interferometry. The main advantage of kaons is that only the $K^*(892)$ with a modest $1/\Gamma \approx 4$ fm/c is an important source of kaons. At higher SPS energies it is know experimentally, and the Lund model correctly accounts for the fact that about 1/2 of the kaons are decay products of that resonance. However, the long lived ω, η, η' that plague the pion production are absent in the kaon channel.

On the other hand a disadvantage of kaon interferometry is the large Coulomb hole $\propto m_K$ that leads to $q_c \approx 22$ MeV. Therefore, the Coulomb correction is much large and the true signal has to be extracted from a deeper hole. In addition, because the $K/\pi < 0.25$, the statistics of kaon pairs is much lower than for pions. As seen in Fig 1, even high statistics of pion pairs data are not yet sufficient accurate to differentiate widely differing dynamical models. Nevertheless, as a complementary probe, kaon pairs provide valuable additional constraints.

One of the novel feature of kaon interferometry is that K_s can used instead of $K^\pm$. In [5], it was shown that $K_s - K_s$ interferometry is sensitive a new interference term that could be used to search for strangeness distillation phenomena in high energy nuclear reactions. The main physics motivation[11, 12], is that a system at finite baryon densities may under certain conditions distill strange quarks by evaporating K^+ and K_0 preferentially to K^- and $\overline{K}_0$. In a quark-gluon plasma strangeness, distillation could occur if the chemical potential of light quarks exceeds the strange quark mass. In a baryon rich hadronic gas, the difference between $\sigma(K^+p) \sim 10$ mb and $\sigma(K^-p) \sim 50$ mb for $p_{rel} \lesssim 1$ GeV can cause a slower diffusion of the negative strangeness in high baryon density matter[12]. In either case, one expects a relative time delay between the K_0 and $\overline{K}_0$ emission.

The new twist in neutral kaon interferometry is that the strong interaction dynamics are diagonal in the strangeness basis while the weak interactions are not. Thus, in the

asymptotic CP eigenstates the relevant two kaon density matrix is a linear combination of density matrices for different strangeness eigenvalues:

$$\langle K_s K_s || f_2 || K_s K_s \rangle = \frac{1}{4}(f_{++} + f_{+-} + f_{-+} + f_{--}) \ , \tag{17}$$

where $\pm$ refers to the strangeness quantum number. As a result the interference pattern depends on both ***decoupling*** distributions $D_+(x,p)$ and $D_-(x,p)$ of the K_0 and $\overline{K}_0$ respectively. Defining the reduced (Gamow corrected) identical kaon correlation function

$$R_a(q,K) = C_a(k_1,k_2)/\chi_a(q) - 1 \ , \tag{18}$$

where $a = s, +, -$ for $K_s K_s$, K^+K^+, and K^-K^-, resp., and $\chi_s = 1$, $\chi_\pm = (q_c/q)/(e^{q_c/q} - 1)$ is the Gamow factor with $q_c = 2\pi\alpha m_K$, we find that

$$\begin{aligned} R_\pm(q,K) &= |D_\pm(q,K)|^2/(D_\pm(0,k_1)D_\pm(0,k_2)) \ , \\ R_s(q,K) &= f(k_1)f(k_2)R_+(q,K) + (1-f(k_1))(1-f(k_2))R_-(q,K) \\ &\quad +2f(k_1)(1-f(k_2))I_{+-}(q,K) \ . \end{aligned} \tag{19}$$

The local K^+ fraction is the ratio of single inclusive cross sections given by

$$f(k) = D_+(0,k)/D(0,k) = K^+/(K^+ + K^-) = K_0/(K_0 + \overline{K}_0) \ , \tag{20}$$

and the new interference term is

$$I_{+-}(q,K) = Re(D_+(q,K)D_-(-q,K))/(D_+(0,k_1)D_-(0,k_2)) \ . \tag{21}$$

For high baryon densities, we expect $f = 1 - \epsilon$, where $\epsilon \approx K^-(k_\perp)/K^+(k_\perp) \ll 1$. To first order in ϵ for example,

$$R_s(q,K) \approx (1-2\epsilon)R_+(q,K) + 2\epsilon e^{-q_\perp^2(r_+^2+r_-^2)/4}(1 - \tfrac{1}{2}(\tau_+^2 T_+ + \tau_-^2 T_-)m_\perp(y_1 - y_2)^2) \ . \tag{22}$$

This shows that the K_s correlation function may have a two component structure if strangeness distillation occurs. One component is just R_+ suppressed by the factor $1 - 2\epsilon$, and the other depends on the decoupling parameters of both strangeness and anti-strangeness.

The most suitable energy range for such studies is $E_{lab} \sim 10 - 15$ AGeV (at the AGS) where maximal baryon densities are likely to be achieved in $Au + Au$ collisions. At these energies, $\epsilon = K^-/K^+ \sim 0.2$ so that more conventional K^-K^- interferometry is much more difficult than K^+K^+. In this case $K_s K_s$ interferometry may be the only practical way to get a glimpse of the anti-strangeness decoupling distribution.

Acknowledgements: We are grateful for the support and hospitality of the nuclear theory group at LBL, where this work was initiated. Extensive discussions with R. Morse, S. Nagamiya, and W. Zajc are also gratefully acknowledged.

References

[1] M. Gyulassy, S. S. Padula, Phys. Lett. 217B (1989) 181.

[2] S.S. Padula, M. Gyulassy, and S. Gavin, Nucl. Phys. B329 (1990) 357.

[3] S. S. Padula and M. Gyulassy, Nucl. Phys. B339 (1990) 378.

[4] M. Gyulassy and S.S. Padula, Phys. Rev. C41 (1990) R21.

[5] M. Gyulassy, Phys. Lett.Phys.Lett.B286:211-215,1992.

[6] T. Abbott, et al (E802 Collab.), Phys. Rev. Lett. 69 (1992) 1030.

[7] G. Bertsch, M. Gong, M. Tohyama, Phys. Rev. C37 (1988) 1896.

[8] B. Andersson, et al., Nucl. Phys. B281 (1987) 289;
M. Gyulassy, CERN-TH.4794 (1987), published in Proc. Eight Balaton Conf. on Nucl. Phys. (ed. Z. Fodor, KFKI, Budapest 1987).

[9] V. Blobel, et al,Phys. Lett. 48B (1974) 73.

[10] T. Abbott et al (E802 collab) Phys. Rev. Lett., 64 (1990) 847; Phys. Rev. Lett. 66 (1991) 1567.

[11] C. Greiner , B. Muller Phys. Lett. B219 (1989) 199.

[12] U. Heinz , K.S. Lee, M.J. Rhoades-Brown Mod. Phys. Lett. A2 (1987) 153; Phys. Rev. Lett. 58 (1987) 2292.

[13] R.J. Morse, MIT thesis 1990, Nucl.Phys. A525 (1991) 531c ; W. Zajc, Proc. QM91.

5 Figure Captions

Fig. 1 Negative pion correlations in central Si+Au reactions[6] as a function of transverse momentum difference Q_T. Parts (a,b) show data corrected for acceptance but uncorrected for Coulomb and calculations including the Gamow factor. Parts (c,d) show data corrected for Coulomb vs theory without Gamow. All calculations refer to a decoupling phase space density parametrized as in Eq. (8). Parts (a,d) correspond to $R_T = 3.5$ and $\tau \equiv \Delta\tau = 2$ fm. Parts (b,d) correspond to $R_T = \tau = 4.6$ fm. In all cases the correlations resulting from symmetrizing dynamics with (1) no resonance (top histogram) (2) 1/10 Lund resonance fraction (dot-dashed histogram) and (3) Full Lund resonance fractions (lower solid histograms) are shown.

Fig. 2 Upper panel shows Coulomb and acceptance corrected 2D data[6, 13] on $C(q_\perp, q_L)$. Right axis is $q_\perp$ in GeV/c, and left axis is q_L. Lower panel shows corresponding lego plot for the expected correlation function corresponding to the decoupling distribution Eq.(8), with $R_T = \tau = 4.6$ fm and assuming no resonance production.

Fig. 3 (a) 2D χ^2 comparison of top and bottom lego plots in Fig. 2. The χ^2 per bin is the square of the difference between theory and data divided by the square of the quoted experimental error (not shown above). Note the huge ridge of very poor fit along $q_L \approx q_\perp$.

(b) Improved χ^2 comparison including a linear tilt degree of freedom in the $(q_L, q_\perp)$ plane with tilt parameters determined to minimize the global χ^2. The ridge is reduced but the overall fit remains poor.

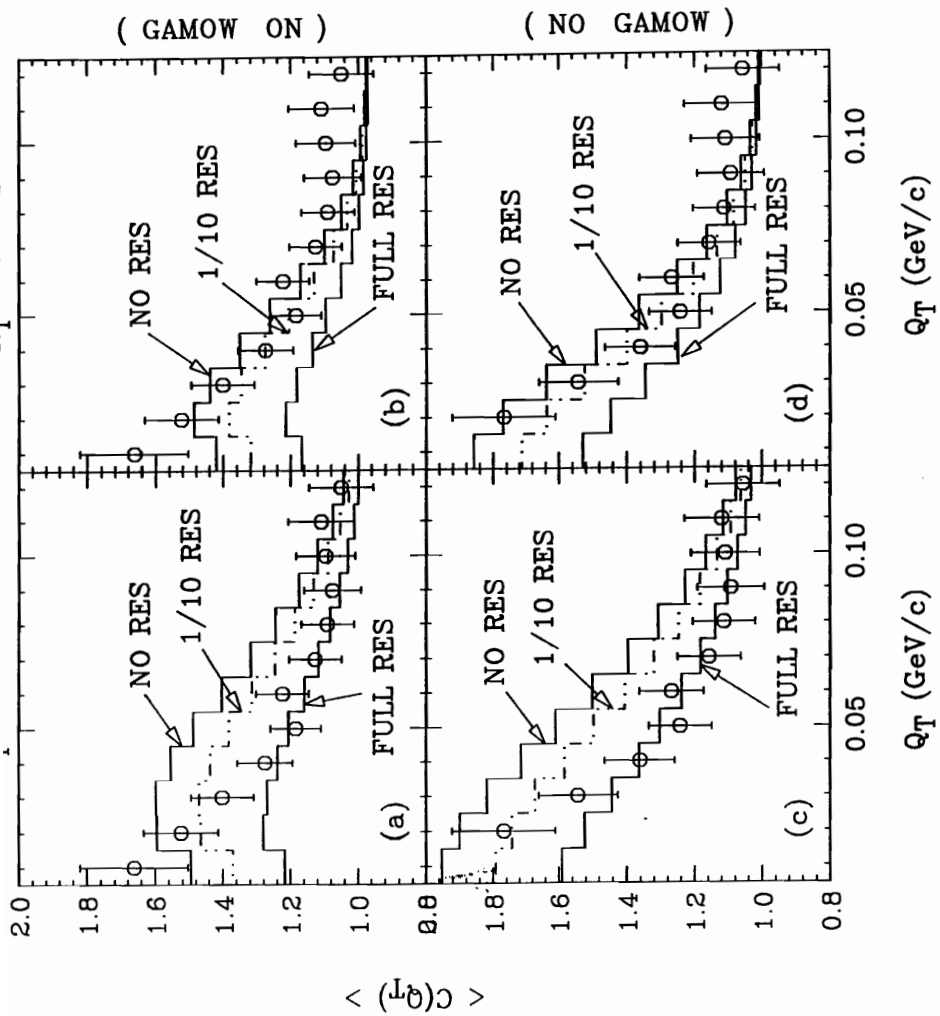

Fig. 1

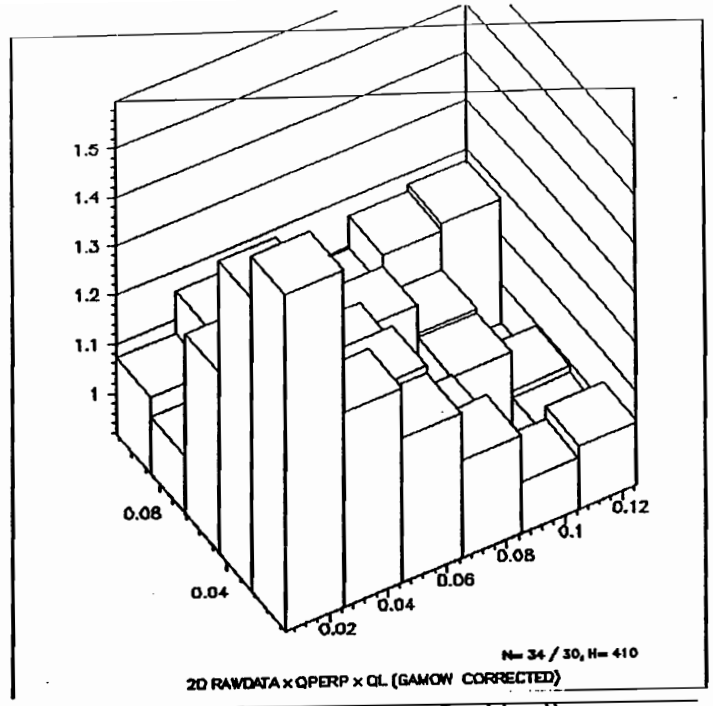

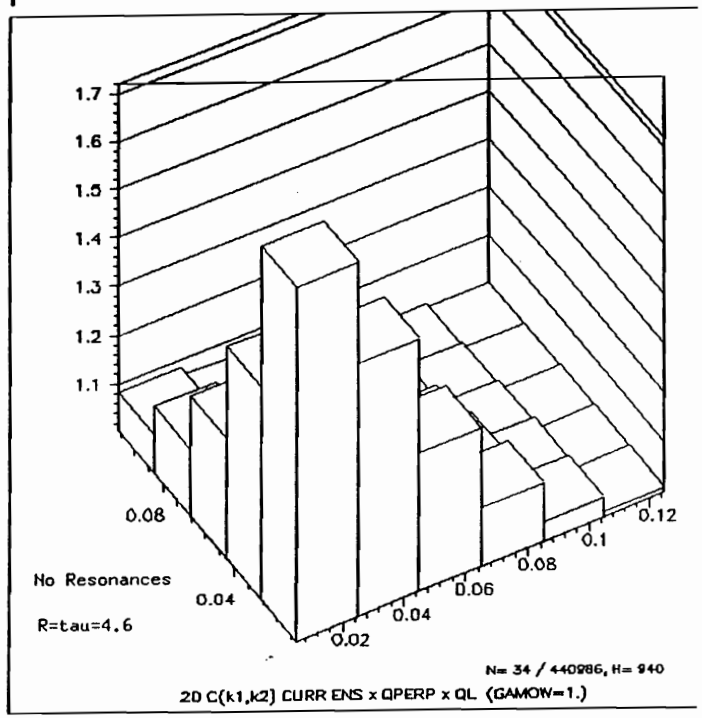

Fig.2 p.12

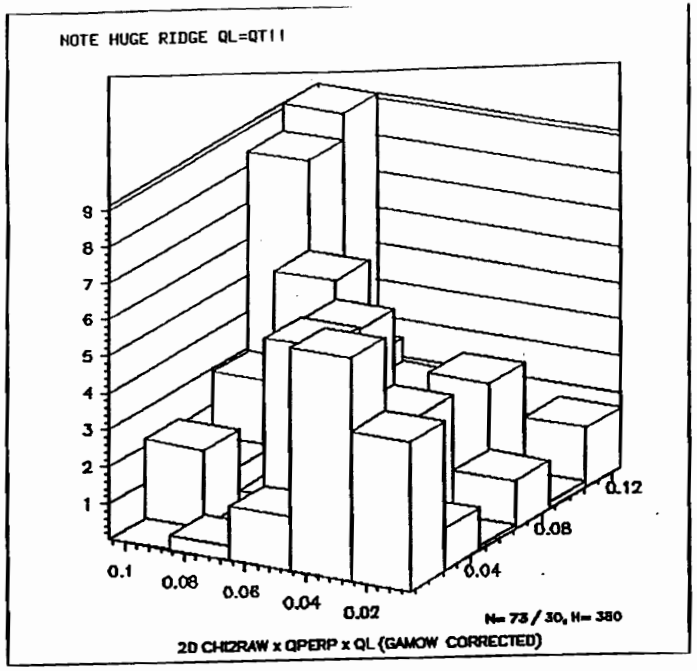
NOTE HUGE RIDGE QL=QT!!
9
8
7
6
5
4
3
2
1
0.1
0.08
0.06
0.04
0.02
0.04
0.08
0.12
N= 73 / 30, H= 380
2D CHI2RAW x QPERP x QL (GAMOW CORRECTED)

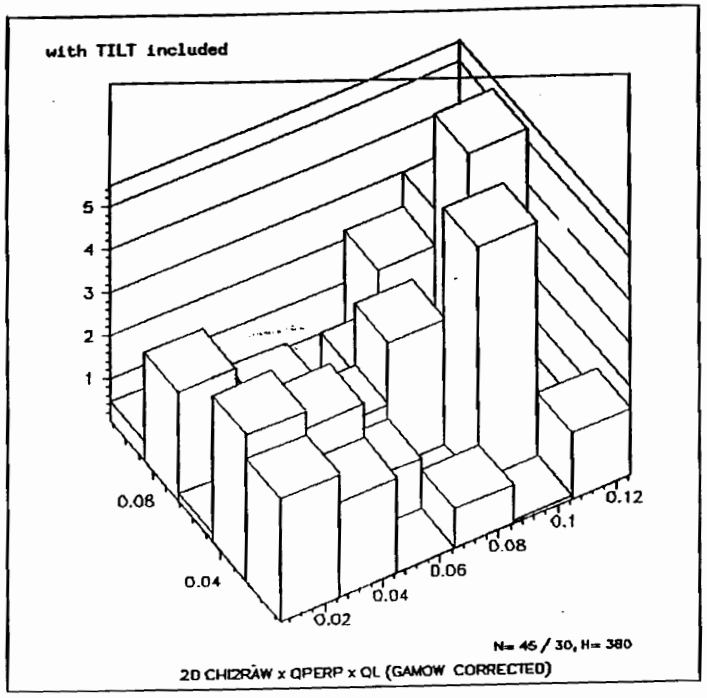
with TILT included
5
4
3
2
1
0.08
0.04
0.02
0.04
0.06
0.08
0.1
0.12
N= 45 / 30, H= 380
2D CHI2RAW x QPERP x QL (GAMOW CORRECTED)

Fig.3 p13